

1 Article

2 **Transcriptome Profiling Reveals Inhibitory Effect of Down-regulated ZBTB38 gene on**
3 **the Transcriptional Regulation of Tumor Cells Proliferation**

4 Jie Chen^{*, †, ‡}, Chaofeng Xing^{*, †, 1}, Haosen Wang[§], Zengmeng Zhang^{*}, Daolun Yu^{*}, Jie Li^{*},
5 Honglin Li^{**}, Jun Li^{*2}, Yafei Cai^{*, †, 2}

6 ^{*} College of Life Sciences, Anhui Provincial Key Lab of the Conservation and Exploitation of Biological
7 Resources, Anhui Normal University, Wuhu 241000, China; chenjie1006@foxmail.com (J.C.);
8 1820491215@qq.com (C.X.); 386170564@qq.com (Z.Z.); 13965466460@126.com (D.Y.);
9 1660700720@qq.com (J.L.)

10 [†] College of Animal Science and Technology, Nanjing Agricultural University, Nanjing 210095, China

11 [‡] The Secondary Hospital of Wuhu, Wuhu 241000, China

12 [§] Taizhou 4th Hospital, Taizhou 235300, China; billet_wang@163.com (H.W.)

13 ^{**} Department of Biochemistry and Molecular Biology, Medical College of Georgia, Augusta
14 University, Augusta, GA 30912, USA; hli@gru.edu (H.L.)

15 ¹ Co-first author

16 ² Correspondence: College of Life Sciences, Anhui Normal University, No.1 BeiJing East Road, Wuhu,
17 Anhui province, P. R. China, 241000; ycai@njau.edu.cn (Y.C.); lijunplant@163.com (J.L.) Tel.:
18 +86-553-386-9297

19 **Abstract:** Transcription factor ZBTB38 belongs to the zinc finger protein family and
20 contains the typical BTB domains. Only several predicted BTB domain-containing proteins
21 encoded in the human genome have been functionally characterized. No relevant studies
22 have been reported concerning the effect of down-regulated ZBTB38 gene expression on
23 tumor cells through transcriptome analysis. In the present study, 2,438 differentially
24 expressed genes in ZBTB38^{-/-} SH-SY5Y cells were obtained via high-throughput
25 transcriptome sequencing analysis, 83.5% of which was down-regulated. Furthermore, GO
26 functional clustering and KEGG pathway enrichment analysis of these differentially

27 expressed genes (DEGs) revealed that the knocked-down transcription factor ZBTB38
28 interacted with p53 and arrested cell cycles to inhibit the proliferation of the tumor cells.
29 Besides, it also significantly down-regulated the expressions of PTEN, a "molecular switch"
30 of the PI3K/Akt signaling pathway, and RB1CC1, the key gene for autophagy initiation,
31 and blocked autophagy to accelerate the apoptosis of tumor cells. ZBTB38^{-/-} SH-SY5Y
32 cells were investigated at the whole transcriptome level and key DEGs were screened in the
33 present study for the first time, providing a theoretical foundation for exploring the
34 molecular mechanism of inhibition of tumor cell proliferation and targeted anti-tumor
35 therapies.

36 **Keywords:** ZBTB38; transcriptome; DEGs; SH-SY5Y; RNA sequencing

37 **Introduction**

38 The zinc finger and BTB domain-containing protein family (ZBTB) is a class of
39 regulatory proteins that contain multiple C2H2 or C2HC zinc finger domains at the
40 C-terminus and BTB domains at the N-terminus. Most members of the family, as
41 transcription factors, bind to specific DNA sequences and regulate the transcriptional activity
42 of target genes(Stogios et al. 2005; Sasai et al. 2005). In addition, the family members also
43 involve in various intracellular signal transduction pathways via recognizing and interacting
44 with other proteins, thereby playing important roles in the transcriptional repression, DNA
45 damage, tumorigenesis, and cell proliferation, differentiation, and apoptosis(Lee and Maeda
46 2012; Matsuda et al. 2008; Nishii et al. 2012).

47 At least 49 ZBTB proteins are encoded in the human genome, most of which are nuclear
48 proteins (Lee and Maeda 2012). The ZBTB38 (also known as CIBZ) belongs to the human
49 zinc finger protein gene family with typical BTB domains. Among the predicted BTB
50 domain-containing proteins encoded by the human genome, only several of them have been
51 functionally characterized (Matsuda et al. 2008; Cai et al. 2012). The present study was

52 designed to analyze the effect of down-regulated expression of ZBTB38 gene on tumor cells
53 in vitro by transcriptome analysis using the neuroblastoma cell model with down-regulated
54 ZBTB38 gene which was successfully established in our previous study s study (Cai et al.
55 2012; Cai et al. 2017). Consequently, it was found for the first time that when exogenous
56 genes were inserted into the exogenous gene via liposomes, autophagy was not initiated to
57 regulate the protective mechanism of the stress response, which was blocked on the contrary.

58 Research of the ZBTB protein family is currently focused on the process of tumor
59 formation and infections. However, it is rarely reported with respect to the effect of ZBTB38
60 on the level of transcriptome of tumor cells. Transcriptomic studies are developing rapidly
61 over recent years, which, contrary to the studies on an individual gene, enable the
62 investigation on the altered expression of differentially expressed genes (DEGs) on the level
63 of whole protein-coding or non-coding RNAs in cells or tissues of the body. Besides, it can
64 also provide information of the relationship between transcriptional regulation and the
65 protein functions in the whole genome under specific conditions (Zhao et al. 2011; Reimann
66 et al. 2014). The development of RNA sequencing (RNA-seq) technology offers important
67 technical support for the annotation and quantification of transcriptomes. The major strength
68 of this technique lies in its high-throughput and high sensitivity for transcript abundance,
69 providing throughout understanding of the transcriptional information of the genome in a
70 comprehensive manner (Chang et al. 2015; Li et al. 2014).

71 To understand the effect of down-regulated ZBTB38 gene on the transcriptional
72 regulation of tumor cells proliferation, a high-throughput transcriptome sequencing
73 (RNA-seq) approach was adopted to investigate the transcriptome profiles of neuroblastoma
74 cells in which the expression of ZBTB38 gene was down-regulated. Furthermore, DEGs
75 were subjected to bioinformatics analysis of functional clustering with GO annotation and
76 pathway enrichment with KEGG pathway database. Key DEGs were screened and verified
77 by quantitative RT-PCR to obtain more important regulatory genes involved in tumor

78 formation regulated by the transcription factor ZBTB38 and to understand the related
79 regulatory mechanisms, providing a theoretical basis for further exploration of targeted
80 anti-tumor therapies.

81 **Materials and Methods**

82 *Cell culture and standard assays*

83 SH-SY5Y cells were purchased from American Type Culture Collection (Rockville,
84 MD, USA) and cultured in Dulbecco's modified Eagle's medium supplemented with 10%
85 fetal bovine serum and penicillin–streptomycin. Transient transfections, quantitative
86 real-time polymerase chain reaction (qRT-PCR) were performed as described previously
87 (Cai et al. 2012; Cai et al. 2017). The primers used in qRT-PCR and siRNA suppression
88 assays are listed in supplemental Table S1.

89 *RNA Preparation and library construction for transcriptome sequencing*

90 Transcriptome high-throughput sequencing was performed in the control group
91 (SH-SY5Y cells transfected with liposome alone, Samples-ID: T04, T05, T06) and the
92 treatment group (SH-SY5Y cells transfected with ZBTB38 siRNA, Samples-ID: T01, T02,
93 T07). Total RNA was isolated from SH-SY5Y cells using TRIzol and the pure-link RNA
94 mini kit (ThermoFisher Scientific, Waltham, MA, USA) according to manufacturer's
95 instructions. RNA purity was checked using the NanoPhotometer spectrophotometer
96 (IMPLEN, CA, USA). RNA concentration was measured using the Qubit RNA Assay Kit
97 in Qubit 2.0 Fluorometer (Life Technologies, CA, USA). RNA integrity was assessed using
98 the RNA Nano 6000 Assay Kit of the Agilent Bioanalyzer 2100 system (Agilent
99 Technologies, CA, USA).

100 A total amount of 2 μ g RNA per sample was used as input material for the RNA
101 sample preparations. This study included two groups of three biological replicates.

102 Sequencing libraries were generated using NEBNext UltraTM RNA Library Prep Kit for
103 Illumina (NEB, USA) and index codes were added to attribute sequences to each sample.
104 Fragmentation was carried out using divalent cations under elevated temperature in
105 NEBNext First Strand Synthesis Reaction Buffer (5X). First strand cDNA was synthesized
106 using random hexamer primer and M-MuLV Reverse Transcriptase (RNase H-). Second
107 strand cDNA synthesis was subsequently performed using DNA Polymerase I and RNase H.
108 Remaining overhangs were converted into blunt ends via exonuclease/polymerase activities.
109 After adenylation of 3' ends of DNA fragments, NEBNext Adaptor with hairpin loop
110 structure were ligated to prepare for hybridization. The library fragments were purified with
111 AMPure XP system (Beckman Coulter, Beverly, USA). Then PCR was performed with
112 Phusion High-Fidelity DNA polymerase, Universal PCR primers and Index (X) Primer. At
113 last, PCR products were purified (AMPure XP system) and library quality was assessed on
114 the Agilent Bioanalyzer 2100 system. The clustering of the index-coded samples was
115 performed on a cBot Cluster Generation System using the TruSeq PE Cluster Kit
116 v4-cBot-HS (Illumina). Following cluster generation, the library preparations were
117 sequenced on an Illumina Hiseq 2500 platform, and paired-end reads were generated.

118 *4.3 Data and Statistical Analysis*

119 *4.3.1 Quality control*

120 Raw reads of fastq format were firstly processed through in-house perl scripts. In this
121 step, clean reads were obtained by removing reads containing adapter, reads containing
122 ploy-N and low quality reads from raw reads. At the same time, Q20, Q30, GC-content and
123 sequence duplication level of the clean reads were calculated. All the downstream analyses
124 were based on clean reads with high quality (Ewing and Green 1998; Ewing et al. 1998).
125 The clean data of this article are publicly available in the NCBI Sequence Reads Archive
126 (SRA) with accession number SRP150042.

127 4.3.2 Comparative analysis

128 The adaptor sequences and low-quality sequence reads were removed from the data
129 sets. Raw sequences were transformed into clean reads after data processing. These clean
130 reads were then mapped to the reference genome sequence. Only reads with a perfect match
131 or one mismatch were further analyzed and annotated based on the reference genome.
132 Tophat2 tools soft were used to map with reference genome (Langmead et al. 2009; Kim et
133 al. 2013). Reference genome download address:
134 ftp://ftp.ensembl.org/pub/release-80/fasta/homo_sapiens/.

135 4.3.3 Gene functional annotation

136 The assembled sequences were compared against the NR(NCBI non-redundant protein
137 sequences), Nt (NCBI non-redundant nucleotide sequences), Pfam ([Protein family](#)),
138 Swiss-Prot, KOG/COG ([Clusters of Orthologous Groups of proteins](#)), Swiss-Prot ([A](#)
139 [manually annotated and reviewed protein sequence database](#)), KO ([KEGG Ortholog](#)
140 [database](#)), and GO ([Gene Ontology](#)) databases with an E-value $\leq 10^{-5}$ for the functional
141 annotation. The Blast2GO program was used to obtain GO annotation of unigenes
142 including molecular function, biological process, and cellular component categories (Gotz
143 et al. 2008).

144 4.3.4 Differential expression analysis

145 Differential expression analysis of the two conditions was performed using the
146 DEGseq R package(Robinson et al. 2010). The P-values obtained from a negative binomial
147 model of gene expression were adjusted using Benjamini and Hochberg corrections to
148 control for false discovery rates (Anders and Huber 2010). Genes with an adjusted P-value
149 < 0.05 were considered to be differently expressed between groups. DEG expression levels

150 were estimated by fragments per kilobase of transcript per million fragments
151 mapped(Florea et al. 2013). The formula is shown as follow:

$$152 \quad \text{FPKM} = \frac{\text{cDNA Fragments}}{\text{Mapped Fragments(Millions)} \times \text{Transcript Length(kb)}}$$

153 4.3.5 GO enrichment and KEGG pathway enrichment analysis

154 GO enrichment analysis of the differently expressed genes (DEGs) was implemented in
155 the “Goseq” package in R based on a Wallenius non-central hyper-geometric distribution,
156 which can adjust for gene length bias in DEGs(Young et al. 2010).

157 KEGG is a database for understanding high-level functions and utilities of biological
158 systems through large-scale molecular datasets generated by genome sequencing and other
159 high-throughput experimental technologies (<http://www.genome.jp/kegg/>) (Kanehisa et al.
160 2008). We used the KOBAS software to test for the statistical enrichment of differentially
161 expressed genes in KEGG pathways. KEGG enrichment can identify the principal
162 metabolic pathways and signal transduction pathways of DEGs (Mao et al. 2005).

163 4.3.6 DEGs quantitative real-time pcr (qRT-PCR) verification

164 For validation of the transcriptome result, we subjected three significantly differential
165 expressed unigenes on related pathways to qRT-PCR analysis. Redundant RNA from the
166 cDNA library preparation was used to perform reverse transcription according to the
167 Invitrogen protocol. quantitative real-time polymerase chain reaction (qRT-PCR) were
168 performed as described previously (Zhang et al. 2017). The primers used in qRT-PCR
169 suppression assays are listed in Table 1.

170 4.3.7 Statistical analysis

171 All data were reported as mean \pm standard deviation and analyzed using one-way
172 analysis of variance in SPSS v.17.0. Statistical tests were performed with the

173 Kruskal–Wallis and Mann–Whitney U-tests. A least significant difference test was used for
174 comparisons between groups. A P-value < 0.05 was considered statistically significant.

175 **2. Results**

176 *2.1 Quality control and yield statistics of transcriptome sequencing data*

177 A total of 47.05 Gb clean data were obtained through the transcriptome sequencing of
178 SH-SY5Y cells, with at least 6.12 Gb and a \geq 89.30% Q30 percentage for each sample (Table
179 1). Efficiency of sequence alignment referred to the percentage of mapped reads in the clean
180 reads, which reflected the utilization of transcriptome sequencing data. Statistical analysis of
181 the alignment results showed that the efficiency of read alignment for the reads of each
182 sample and the reference genome ranged between 79.42% and 81.92% (Table 2), which
183 guaranteed that the selected reference genome assembly was qualified for data analysis.

184 **Table 1.** Summary of Illumina transcriptome sequencing for ZBTB38^{-/-} cells

Samples-ID	Clean reads	Clean bases	GC Content	% \geq Q30
T01	20,660,153	6,116,098,020	56.24%	89.44%
T02	26,853,046	7,955,371,598	55.36%	89.45%
T04	27,444,964	8,143,994,956	52.17%	90.04%
T05	25,080,118	7,422,177,908	52.16%	90.25%
T06	31,360,838	9,309,952,904	51.94%	90.05%
T07	27,346,767	8,098,920,214	55.22%	89.30%

185 **Table 2.** Summary of Sequence comparisons among sample sequencing data and
186 selected reference genomes

Samples-ID	Total Reads	Mapped Reads	Uniq Mapped Reads	Multiple Map Reads
T01	41,320,306	32,993,483 (79.85%)	29,171,906 (70.60%)	3,821,577 (9.25%)
T02	53,706,092	42,655,511 (79.42%)	37,610,672 (70.03%)	5,044,839 (9.39%)
T04	54,889,928	44,964,104 (81.92%)	41,561,590 (75.72%)	3,402,514 (6.20%)
T05	50,160,236	40,559,313 (80.86%)	37,552,835 (74.87%)	3,006,478 (5.99%)
T06	62,721,676	50,526,963 (80.56%)	47,347,475 (75.49%)	3,179,488 (5.07%)
T07	54,693,534	43,544,178 (79.61%)	38,543,679 (70.47%)	5,000,499 (9.14%)

187 Following the counting of mapped reads at different regions (exons, introns, and
188 intergenic regions) of a given reference genome, distribution maps of mapped reads in
189 different regions of the genome were plotted for each sample. Most reads were mapped to the
190 exon regions of the reference transcriptome ($\geq 80\%$ for each) and the alignment results were
191 valid and reliable (see Figure. S1).

192 Qualified transcriptome libraries are a major requisite for transcriptome sequencing. To
193 ensure the quality of the libraries, quality of the transcriptome sequencing libraries was
194 evaluated from three different perspectives:

195 • Randomicity of mRNA fragmentation and the degradation of mRNA were evaluated by
196 examining the distribution of inserted fragments in genes. As shown in Figure S2, the
197 degradation of mRNAs was determined by observing the distribution of mapped reads
198 on mRNA transcripts. The degradation of mRNAs was relatively low in the 6 groups of
199 samples.

200 • Length of the inserted fragments in the transcripts. The length of the inserted fragment
201 was calculated by the distance between the starting and ending sites of the reads flanking
202 the inserted fragment in the reference genome. Due to the fact that no intron regions were
203 available in the transcriptome-sequenced mRNAs, mRNAs in the transcriptome library

204 were more mature if a single peak on the right side of the main peak was noted in the
205 simulated length distribution map of the inserted fragment. By contrast, the alignment
206 length was longer if more interfering peaks appeared showing the intron regions in the
207 inserted fragment. The dispersion degree of the inserted fragment length directly
208 reflected the efficiency of magnetic bead purification during library preparation.
209 Simulated distribution of the inserted fragment length for each sample showed only
210 single-peak pattern, indicating a high purification rate (see Figure. S3).

211 • Sequencing saturation status of DEGs in the mapped data was simulated and plotted for
212 the 6 groups of samples, as graphed in the following map. With the increase of
213 sequencing data, the number of DEGs tended to saturate, as shown in Figure S4, which
214 confirmed that the data were sufficient and qualified for the subsequent analysis.

215 *2.2 DEG and DEGs Function annotation*

216 To acquire the comprehensive genetic information of ZBTB38^{-/-} SH-SY5Y cells, the
217 unigenes were blasted against the NR, Swiss-Prot, GO, COG, KOG, Pfam, KEGG database
218 resources to identify the functions of all of the unigene sequences. All of DEGs were
219 annotated to genes having known functions in the indicated databases based on the sequences
220 with the greatest similarity. DEseq was used to analyze the DEGs derived from the two
221 groups of cells to obtain a DEGs set. Finally, a total of 2,036 (83.5%) down-regulated DEGs
222 and 402 (16.5%) upregulated DEGs were selected. The number of DEGs annotated in this
223 gene set was shown in Table 3.

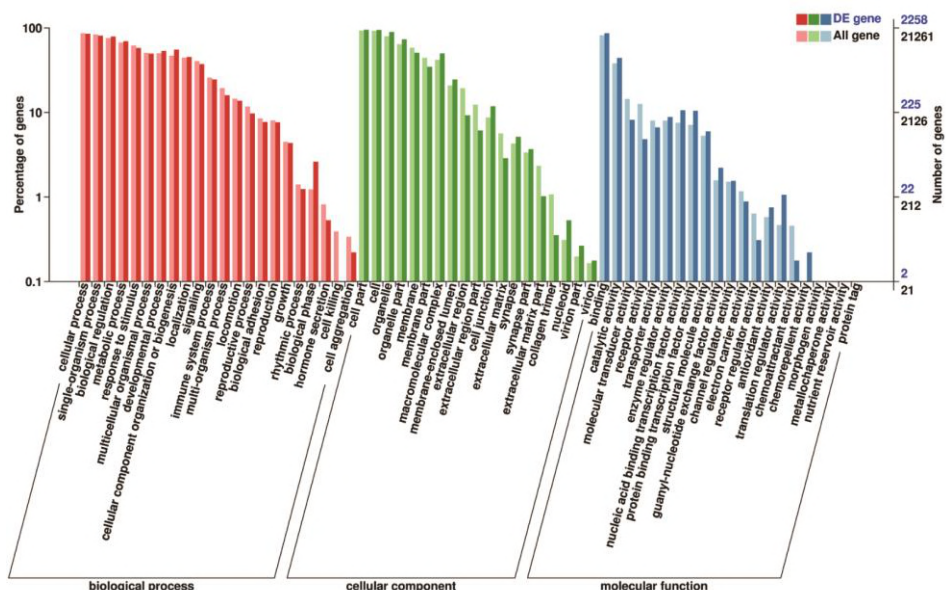
224 **Table 3.** Summary of the function annotation results for ZBTB38^{-/-} unigenes in public
225 protein databases.

DEG Set	Total	COG	GO	KEGG	KOG	NR	Swiss-Prot	eggNOG
---------	-------	-----	----	------	-----	----	------------	--------

T04_T05_T06_vs 2,417 999 2,258 1,512 1,733 2,337 2,377 2,405

_T01_T02_T07

226 A total of 2,258 (93.4%) DEGs were annotated successfully by GO annotation. These
227 annotated DEGs were classified into the next terms of three ontologies: BP (biological
228 process), CC (cellular component) and MF (molecular function). The distribution of
229 unigenes is shown in Figure 1. Among the "Biological Process", a high percentage of genes
230 were classified into "Cellular Process" (1,924 unigenes, 85.2%), "Single-organism Process"
231 (1827 unigenes, 80.9%) and "biological regulation" (1,786 unigenes, 79.1%). Within the
232 cellular component category, the majority of genes were assigned into "Cell Part" (2,145
233 unigenes, 95%) , "Cell" (2,135 unigenes, 94.6%) and "organelle" (2,023 unigenes, 89.6%).
234 For the molecular function, most of genes were involved in "Binding" (1,949 unigenes,
235 86.3%) and "Catalytic Activity" (997 unigenes, 44.2%). The greatest number of annotated
236 unigenes were involved in "Biological Process".

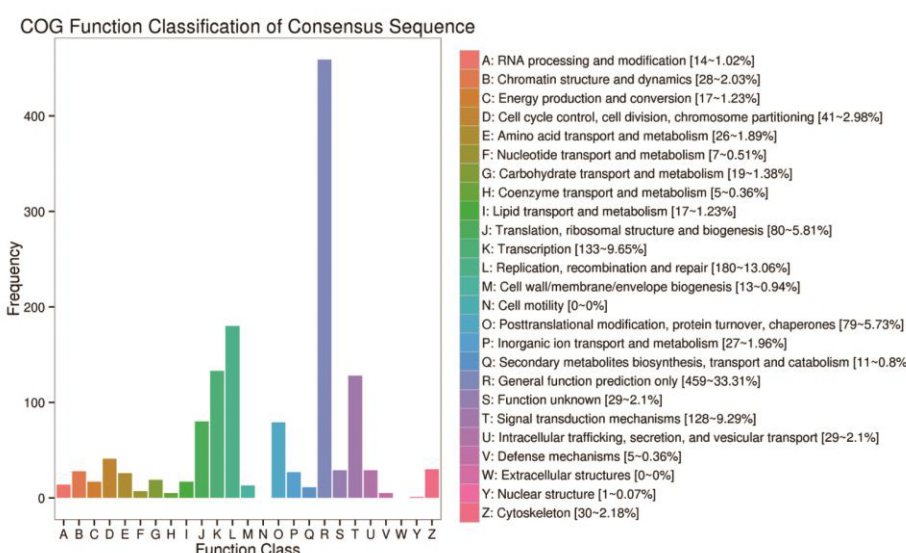


237

238 **Figure 1.** Gene function classification of all annotated unigenes by Gene Ontology.

239 The vertical axis represents the number of unigenes, and horizontal axis gives the
240 specific GO sub-categories.

241 The unigenes was blasted against the COG database in order to orthologously classify
242 gene products. COG classification statistical results of DEGs were shown in Figure 2. In
243 addition to "General function prediction only", "Replication, recombination and repair"
244 accounted for the largest proportion of unigenes(180 DEGs, 13.06%), followed by
245 "Transcription" (133 DEGs, 9.65%), "Signal transduction mechanisms"(128 DEGs, 9.29%),
246 "Translation, ribosomal structure and biogenesis" (80 DEGs, 5.81%), "Posttranslational
247 Modification, Protein Turnover and Chaperones" (79 DEGs, 5.73%), "cell cycle control, cell
248 division, and chromosome partitioning" (44 DEGs, 2.98%).

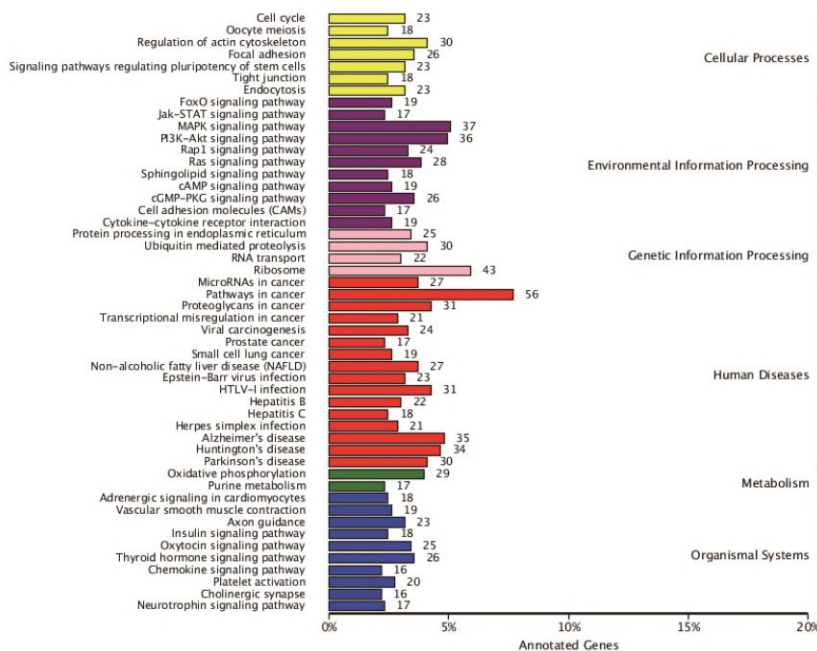


249

250 **Figure 2.** COG function classification of consensus sequence. The vertical axis
251 represents the frequency of unigenes classified into the specific categories, and
252 horizontal axis gives the COG function classification.

253 According to the annotation results of the DEGs KEGG database, KEGG pathways were
254 divided into six branches: "Cellular Processes", "Environmental Information Processing",

255 "Genetic Information Processing", "Human Disease", "Metabolism" and "Organismal
256 Systems"(Figure 3). Among the KEGG categories, the largest proportion of the unigenes
257 were involved in the "MAPK signaling pathway" and "PI3K-Akt signaling pathway" of
258 "Environmental Information Processing", "Regulation of actin cytoskeleton" of "Cellular
259 Processes", and "Ribosomeand" of "Genetic Information Processing".



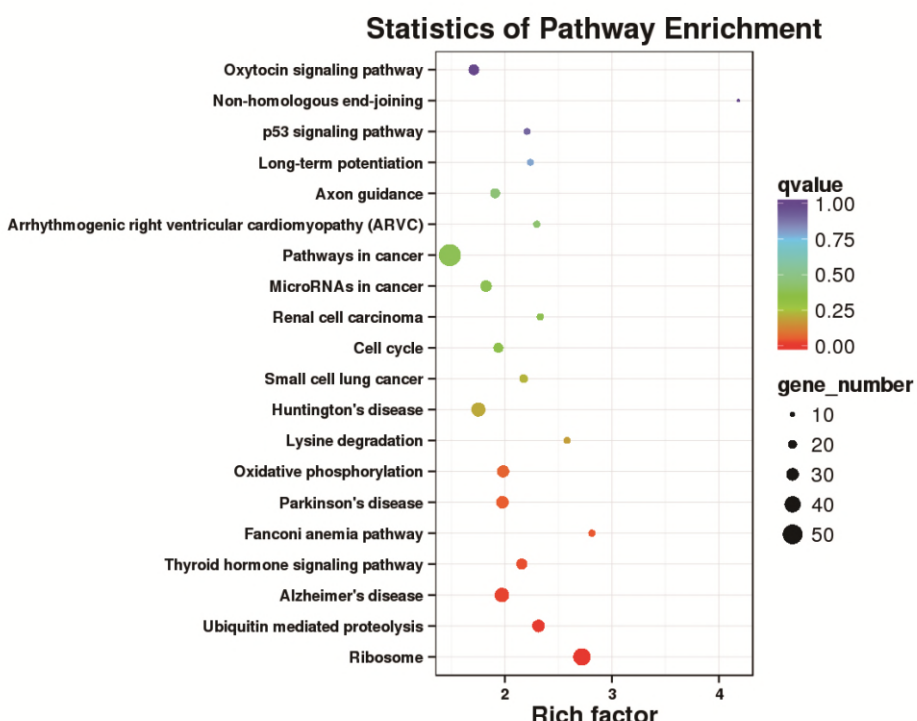
260

261 **Figure 3.** DEG KEGG classification. The vertical axis lists the various metabolic
262 pathways, and horizontal axis gives the percent of annotated genes in the pathways.

263 Based on the results above, a large number of DEGs were screened after a comparative
264 analysis of relevant databases. Meanwhile, functional annotation was also carried out that
265 was crucial for the further understanding of the cellular functions of ZBTB38 gene as a
266 transcription factor.

267 **2.3 DEG KEGG Pathway enrichment and Detection of candidate genes**

268 Pathway enrichment analysis of these DEGs clearly revealed the occurrence of
269 over-presentation of an individual DEG in a given pathway. Pathway enrichment analysis for
270 over-presentation DEGs was performed using the hypergeometric test based on the pathways
271 in the KEGG database to identify pathways that were significantly enriched for DEGs
272 compared to the whole-genome background signals. The results of the KEGG pathway
273 enrichment analysis of DEGs were presented in the figure below, showing the top 20
274 pathways with the smallest significant q-values (Figure 4). Generally, the largest number of
275 DEGs was enriched in the pathway of "Ribosome", 39 DEGs were up-regulated and 1 DEG
276 was down-regulated. The results indirectly indicated that in the ZBTB38^{-/-} cells, the function
277 of protein synthesis increased significantly.



278

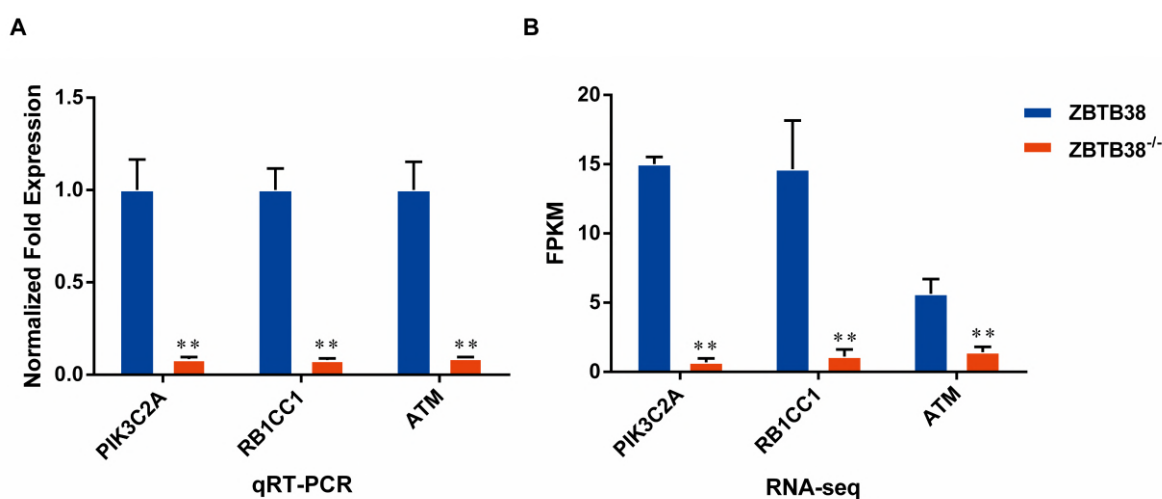
279 **Figure 4.** Scatter plot of the KEGG pathway enrichment analysis for DEGs. Each
280 circle in the graph represented a KEGG pathway, with the name of the pathway in
281 the Y-axis and the enrichment factor in the X-axis. An enrichment factor was
282 calculated as the ratio of the proportion of DEGs annotated to a given pathway in all
283 DEGs to the proportion of all genes annotated to the same pathway in all genes. A

284 greater enrichment factor indicated a more significant enrichment of the DEGs in a
285 given pathway. The color of the circle represented the q-value which was the
286 adjusted P after multiple hypothesis testing. A smaller q-value indicated a higher
287 reliability of the significance of the enrichment of DEGs in a given pathway. The
288 size of the circle indicated the number of genes enriched in the pathway, with bigger
289 circle for more genes enriched.

290 In the KEGG Pathway enrichment analysis, quantification of transcripts and gene
291 expression levels were achieved by Cuffquant and Cuffnorm programs from the Cufflinks
292 software package using the location of a given mapped read on these genes for the 6 groups
293 of samples. Taking FPKM as a measure for the level of transcripts or gene expressions, top
294 20 down-regulated unigenes associated with autophagy were selected (see Table S2), among
295 which PIK3C2A was the most down-regulated one, followed by RB1CC1 gene. Genes,
296 including RB1CC1, DDR2, ATM, and FRK, were related to the mTOR signaling pathway
297 and located in the downstream of PI3K-Akt signaling pathway. In summary, the transcription
298 factor ZBTB38 is involved in the process of protein synthesis and also, as a positive
299 regulatory factor, in the occurrence of autophagy directly.

300 *2.4 Analysis of the results of Real-time quantitative PCR*

301 To validate the sequencing results obtained by RNA-seq, real-time quantitative PCR was
302 performed on three candidate genes, including PIK3C2A, RB1CC1, ATM, related to the
303 mTOR signaling pathway. The result showed that the expression of these candidate genes
304 was significantly decreased in the ZBTB38^{-/-} cells compared to control group, which was
305 similar to the RNA-seq data (Figure 5). The result verified the reliability of the transcription
306 sequencing results.



307

308 **Figure 5.** Differential expression analysis of candidate genes between ZBTB38
309 knockdown (ZBTB38^{-/-}) and wild-type SH-SY5Y cells (ZBTB38). (A) The result of
310 qRT-PCR. (B) The result of RNA-seq.

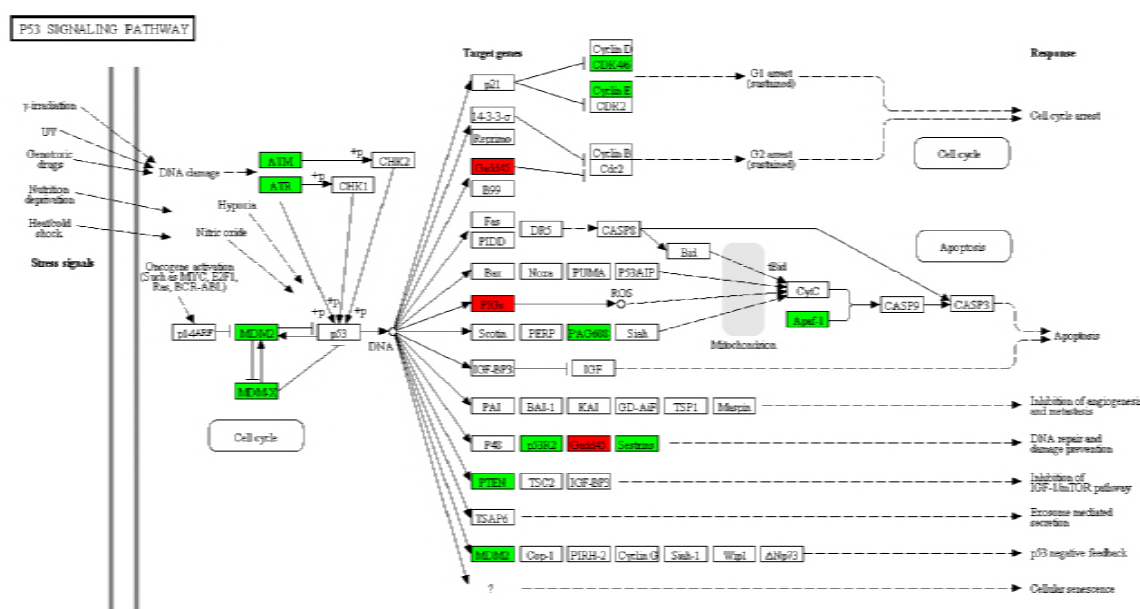
311 3. Discussion

312 Transcriptomic studies are developing rapidly over recent years. Broadly speaking, the
313 transcriptome is defined as the sum of genes expressed by a single cell or cells group under
314 certain conditions, including the mRNAs, rRNAs, miRNAs, and ncRNAs. In a narrow sense,
315 the transcriptome refers only to the protein-coding mRNAs. The level and pattern of gene
316 expression are different in the body at different growth environment and growth stage, with
317 specific temporal and spatial features, and regulated by both endogenous and exogenous
318 factors. Based on the information of the whole mRNAs obtained in one cell or tissue,
319 transcriptomic studies provide data on the expression regulation systems and protein
320 functions of all genes. Simultaneously, the development of RNA-seq technique offers
321 important technical support for the annotation and quantification of the transcriptome. This
322 research method based on the whole genome of organisms has completely transformed the
323 approach that single-gene study works (Wang et al. 2009; Young et al. 2010; McGettigan
324 2013).

325 Among the predicted BTB domain-containing proteins encoded in the human genome,
326 only several of them have been functionally characterized (Lee and Maeda 2012). In the
327 present study, the KEGG pathway enrichment analysis of DEGs revealed that genes in the
328 p53 signaling pathway, including CDK4/6, Cyclin E, MDM2, ATM, ATR, PTEN, were
329 down-regulated, and Gadd45 and PIGs were up-regulated after the knockdown of ZBTB38
330 (Figure 6). Both the CDK4/6-Cyclin D and the CDK2-Cyclin E complexes are the central
331 links in cell cycle regulation via regulating the G1-S transitions in cells, and abnormal
332 activation of the CyclinD-CDK4/6-INK4-Rb pathway, which is often observed in various
333 malignancies, will lead to uncontrolled growth of cancer cells (The et al. 2015; Sawai et al.
334 2012; VanArsdale et al. 2015). In addition, members of the Gadd45 family serve as key
335 regulatory genes in DNA damage repair pathway with p53 as the central link, and the
336 upregulation of Gadd45 plays an important role in the regulation of G2/M cell cycle
337 checkpoints and the maintenance of genomic stability, therefore to inhibit the cell
338 transformation and the malignant progression of tumors (Wang et al. 2009). ATM and ATR
339 belong to the inositol trisphosphate kinase family, both of which can be activated by DNA
340 damage to phosphorylate the downstream substrates such as CHK1, CHK2, and p53. In
341 addition, the down-regulation of both kinases may impair the downstream transmission of
342 the molecular signals and inhibit the p53 activity (Matsuoka et al. 2007; Abraham 2001).
343 MDM2 regulates the function of p53 via two approaches, i.e., mediating p53 degradation and
344 inhibiting its transcriptional activity. As a negative feedback regulator of p53, the inhibited
345 expression of MDM2 can enhance the transcriptional activity of p53 and inhibit
346 tumorigenesis (Shangary and Wang 2009). PIGs is a target downstream gene of p53 for the
347 regulation of apoptosis, which is critical for cell apoptosis by participating in the synthesis of
348 reactive oxygen species and the regulation of oxidative stress (Jin et al. 2017; Lee et al.
349 2010). When ZBTB38 gene is knocked down, p53 expression is decreased and more PIGs
350 are transferred into the nucleus where cell damage is repaired. Therefore, cellular response to

351 DNA damage is increased and the p53-induced ROS production is reduced, eventually
352 leading to the survival of cells. PTEN is a tumor suppressor gene with phosphatase activity. It
353 is an upstream regulatory inhibitor of the PI3K/Akt signal transduction pathway. PTEN is
354 often referred to as a “switch” molecule in the PI3K/Akt pathway due to its ability, which
355 depends on its lipid phosphatase activity, to remove the phosphate group and participate in
356 the regulation of cell activity. Once the expression of PTEN protein is reduced, the
357 dephosphorylation of PIP3 is decreased. Excessive PIP3 is subsequently accumulated in the
358 cells and the PI3K/Akt signaling pathway is continuously activated, eventually leading to
359 cell proliferation or uncontrolled apoptosis and finally the occurrence of various diseases
360 (Bleau et al. 2009; Carnero et al. 2008). Such interpretation may also explain the findings of
361 the present study that DEGs are mainly enriched in the "PI3K-Akt signaling pathway" of the
362 "Environmental Information Processing" category. In summary, direct effect of
363 down-regulated expression of ZBTB38 on the p53 signaling pathway may provide a novel
364 treatment strategy for targeted anti-tumor therapies.

365



367 **Figure 6.** KEGG pathway annotation map of differentially expressed genes in p53
368 signaling pathway. Relative to the control group, the red box labeled protein was

369 associated with the up-regulated gene and the green box labeled protein was
370 associated with the down-regulated gene.

371 Majority of the DEGs were enriched in the PI3K-Akt signaling pathway among all
372 KEGG pathway enrichment categories, especially for those down-regulated genes, with most
373 significance noted in PIK3C2A and RB1CC1. PIK3C2A is a member of the PI3Ks family
374 and one of the key molecules in the signal transduction pathway of growth factors. It has been
375 reported that the overexpressed PIK3C2A in cells induces the accumulation and assembly of
376 clathrin, which mediates the transport of proteins between cell membranes and the network
377 structure of the Golgi body via regulating the movement of microtubules (Dragoi and
378 Agaisse 2015; Shi et al. 2016). RB1CC1 (also known as FIP200) is an interacting protein of
379 the focal adhesion kinase family, with a molecular weight of 200kD. As documented in prior
380 studies, autophagy induction is abolished in RB1CC1-deficient cells. RB1CC1 is an
381 important regulatory protein that can acts on the autophagic initiation complex along with the
382 ULK1 simultaneously. Besides, it is also a key autophagy initiation factor in the
383 mTORC1-dependent signaling pathway (Wei et al. 2009; Wang et al. 2011; Ganley et al.
384 2009). In addition, significant down-regulation of ATM and FOXO1 genes in the ZBTB38^{-/-}
385 cells was observed by transcriptome sequencing analysis in this study. Ataxia telangiectasia
386 mutated (ATM) belongs to the PIKK (PI3K-related protein kinase) family with C-terminal
387 sequences homologous to that of the catalytic region of PI3K. ATM stimulates the
388 downstream signals of the LBK/AMPK/TSC2 pathway and inhibits the mTORC1 to promote
389 cell autophagy (Alexander et al. 2010; Liu et al. 2013). Members of the forkhead box O
390 (FOXO) family are a group of highly conserved transcription factors that play an important
391 role in the regulation of autophagy (Leger et al. 2006). Therefore, it is believed in our study
392 that the autophagy regulation mechanism of the mTORC1-dependent signaling pathway is
393 also inhibited after ZBTB38 knockdown.

394 Orthologous assignments of gene products were carried out using the COG database.
395 Corresponding statistical analysis of the results also indicated that the silencing of ZBTB38
396 gene affected the homeostasis of the whole cell, and as a transcriptional factor, ZBTB38
397 regulated the transcription of intracellular proteins and influenced the expression and
398 transport of proteins in the downstream signaling pathways. The GO functional enrichment
399 analyses of DEGs suggested that most of the genes were involved in "Binding" and
400 "Catalytic Activity" of the molecular function between ZBTB38^{-/-} cells and the controls.
401 Therefore, this also partially explained the biological functions of the key candidate genes
402 enriched in KEGG pathway, i.e., all of them were specific binding DNAs or proteins that
403 regulated the transcriptional activity of target genes and involved in various intracellular
404 signaling pathways.

405 In conclusion, knockdown of the transcription factor ZBTB38 directly interacted with
406 p53 and arrested cell cycles to inhibit the proliferation of tumor cells. In addition, it also
407 significantly down-regulated the expressions of PTEN, the "molecular switch" of the
408 PI3K/Akt signaling pathway, and RB1CC1, the key gene for autophagy initiation, both of
409 which blocked the autophagy and accelerated the apoptosis of tumor cells. By using
410 neuroblastoma cells, a preliminary study was performed on exploiting DEGs, as well as the
411 key GO terms and KEGG pathways enriched by these DEGs in ZBTB38^{-/-} cells, providing a
412 theoretical foundation for further studies on the regulatory mechanism of ZBTB38 and
413 targeted anti-tumor therapies.

414 **Author Contributions:** Yafei Cai and Jun Li conceived and guided this research. Jie Chen
415 and Chaoxing carried out the experiments, performed data analysis and wrote the manuscript.
416 Haosen Wang and Zengmeng Zhang prepared cell samples and performed the experiments.
417 Daolun Yu and Jie Li performed bioinformatics analysis. Honglin Li analyzed data and

418 discussed results with suggestions from Jie Chen. All authors read and approved the final
419 manuscript.

420 **Acknowledgments:** This study was supported by the National Natural Science Foundation
421 of China (NSFC31372207 and 81570094), the Innovation Team of Scientific Research
422 Platform in Anhui Province, a start-up grant from Nanjing Agricultural University (804090).

423 **Conflicts of Interest:** The authors declare no conflict of interest.

424 References

425 Abraham, R.T., 2001 Cell cycle checkpoint signaling through the ATM and ATR kinases.
426 *Genes Dev* 15 (17):2177-2196. doi:10.1101/gad.914401.
427 <http://www.ncbi.nlm.nih.gov/pubmed/11544175>

428 Alexander, A., S.L. Cai, J. Kim, A. Nanez, M. Sahin *et al.*, 2010 ATM signals to TSC2 in the
429 cytoplasm to regulate mTORC1 in response to ROS. *Proc Natl Acad Sci U S A* 107
430 (9):4153-4158. doi:10.1073/pnas.0913860107.
431 <http://www.ncbi.nlm.nih.gov/pubmed/20160076>

432 Anders, S., and W. Huber, 2010 Differential expression analysis for sequence count data.
433 *Genome Biol* 11 (10):R106. doi:10.1186/gb-2010-11-10-r106.
434 <http://www.ncbi.nlm.nih.gov/pubmed/20979621>

435 Bleau, A.M., D. Hambardzumyan, T. Ozawa, E.I. Fomchenko, J.T. Huse *et al.*, 2009
436 PTEN/PI3K/Akt pathway regulates the side population phenotype and ABCG2
437 activity in glioma tumor stem-like cells. *Cell Stem Cell* 4 (3):226-235.
438 doi:10.1016/j.stem.2009.01.007. <http://www.ncbi.nlm.nih.gov/pubmed/19265662>

439 Cai, Y., J. Li, S. Yang, L. Ping, Z. Xuan *et al.*, 2012 CIBZ, a Novel BTB Domain-Containing
440 Protein, Is Involved in Mouse Spinal Cord Injury via Mitochondrial Pathway
441 Independent of p53 Gene. *PLoS One* 7 (3):e33156.
442 doi:10.1371/journal.pone.0033156.
443 <https://www.ncbi.nlm.nih.gov/pubmed/22427977>

444 Cai, Y., J. Li, Z. Zhang, J. Chen, Y. Zhu *et al.*, 2017 Zbtb38 is a novel target for spinal cord
445 injury. *Oncotarget* 8 (28):45356-45366. doi:10.18632/oncotarget.17487.
446 <http://www.ncbi.nlm.nih.gov/pubmed/28514761>

447 Carnero, A., C. Blanco-Aparicio, O. Renner, W. Link, and J.F. Leal, 2008 The
448 PTEN/PI3K/AKT signalling pathway in cancer, therapeutic implications. *Curr
449 Cancer Drug Targets* 8 (3):187-198.
450 <http://www.ncbi.nlm.nih.gov/pubmed/18473732>

451 Chang, Z., G. Li, J. Liu, Y. Zhang, C. Ashby *et al.*, 2015 Bridger: a new framework for de
452 novo transcriptome assembly using RNA-seq data. *Genome Biol* 16:30.
453 doi:10.1186/s13059-015-0596-2. <http://www.ncbi.nlm.nih.gov/pubmed/25723335>

454 Dragoi, A.M., and H. Agaisse, 2015 The class II phosphatidylinositol 3-phosphate kinase
455 PIK3C2A promotes *Shigella flexneri* dissemination through formation of
456 vacuole-like protrusions. *Infect Immun* 83 (4):1695-1704. doi:10.1128/IAI.03138-14.
457 <http://www.ncbi.nlm.nih.gov/pubmed/25667265>

458 Ewing, B., and P. Green, 1998 Base-calling of automated sequencer traces using phred. II.
459 Error probabilities. *Genome Res* 8 (3):186-194.
460 <http://www.ncbi.nlm.nih.gov/pubmed/9521922>

461 Ewing, B., L. Hillier, M.C. Wendl, and P. Green, 1998 Base-calling of automated sequencer
462 traces using phred. I. Accuracy assessment. *Genome Res* 8 (3):175-185.
463 <http://www.ncbi.nlm.nih.gov/pubmed/9521921>

464 Florea, L., L. Song, and S.L. Salzberg, 2013 Thousands of exon skipping events differentiate
465 among splicing patterns in sixteen human tissues. *F1000Res* 2:188.
466 doi:10.12688/f1000research.2-188.v2.
467 <http://www.ncbi.nlm.nih.gov/pubmed/24555089>

468 Ganley, I.G., H. Lam du, J. Wang, X. Ding, S. Chen *et al.*, 2009 ULK1.ATG13.FIP200
469 complex mediates mTOR signaling and is essential for autophagy. *J Biol Chem* 284
470 (18):12297-12305. doi:10.1074/jbc.M900573200.
471 <http://www.ncbi.nlm.nih.gov/pubmed/19258318>

472 Gotz, S., J.M. Garcia-Gomez, J. Terol, T.D. Williams, S.H. Nagaraj *et al.*, 2008
473 High-throughput functional annotation and data mining with the Blast2GO suite.
474 *Nucleic Acids Res* 36 (10):3420-3435. doi:10.1093/nar/gkn176.
475 <http://www.ncbi.nlm.nih.gov/pubmed/18445632>

476 Jin, M., S.J. Park, S.W. Kim, H.R. Kim, J.W. Hyun *et al.*, 2017 PIG3 Regulates p53 Stability
477 by Suppressing Its MDM2-Mediated Ubiquitination. *Biomol Ther (Seoul)* 25
478 (4):396-403. doi:10.4062/biomolther.2017.086.
479 <http://www.ncbi.nlm.nih.gov/pubmed/28605833>

480 Kanehisa, M., M. Araki, S. Goto, M. Hattori, M. Hirakawa *et al.*, 2008 KEGG for linking
481 genomes to life and the environment. *Nucleic Acids Res* 36 (Database
482 issue):D480-484. doi:10.1093/nar/gkm882.
483 <http://www.ncbi.nlm.nih.gov/pubmed/18077471>

484 Kim, D., G. Pertea, C. Trapnell, H. Pimentel, R. Kelley *et al.*, 2013 TopHat2: accurate
485 alignment of transcriptomes in the presence of insertions, deletions and gene fusions.
486 *Genome Biol* 14 (4):R36. doi:10.1186/gb-2013-14-4-r36.
487 <http://www.ncbi.nlm.nih.gov/pubmed/23618408>

488 Langmead, B., C. Trapnell, M. Pop, and S.L. Salzberg, 2009 Ultrafast and memory-efficient
489 alignment of short DNA sequences to the human genome. *Genome Biol* 10 (3):R25.
490 doi:10.1186/gb-2009-10-3-r25. <http://www.ncbi.nlm.nih.gov/pubmed/19261174>

491 Lee, J.H., Y. Kang, V. Khare, Z.Y. Jin, M.Y. Kang *et al.*, 2010 The p53-inducible gene 3
492 (PIG3) contributes to early cellular response to DNA damage. *Oncogene* 29
493 (10):1431-1450. doi:10.1038/onc.2009.438.
494 <http://www.ncbi.nlm.nih.gov/pubmed/20023697>

495 Lee, S.U., and T. Maeda, 2012 POK/ZBTB proteins: an emerging family of proteins that
496 regulate lymphoid development and function. *Immunol Rev* 247 (1):107-119.

497 doi:10.1111/j.1600-065X.2012.01116.x.
498 <http://www.ncbi.nlm.nih.gov/pubmed/22500835>

499 Leger, B., R. Cartoni, M. Praz, S. Lamon, O. Deriaz *et al.*, 2006 Akt signalling through
500 GSK-3beta, mTOR and Foxo1 is involved in human skeletal muscle hypertrophy and
501 atrophy. *J Physiol* 576 (Pt 3):923-933. doi:10.1113/jphysiol.2006.116715.
502 <http://www.ncbi.nlm.nih.gov/pubmed/16916907>

503 Li, B., N. Fillmore, Y. Bai, M. Collins, J.A. Thomson *et al.*, 2014 Evaluation of de novo
504 transcriptome assemblies from RNA-Seq data. *Genome Biol* 15 (12):553.
505 doi:10.1186/s13059-014-0553-5. <http://www.ncbi.nlm.nih.gov/pubmed/25608678>

506 Liu, Q., C. Xu, S. Kirubakaran, X. Zhang, W. Hur *et al.*, 2013 Characterization of Torin2, an
507 ATP-competitive inhibitor of mTOR, ATM, and ATR. *Cancer Res* 73 (8):2574-2586.
508 doi:10.1158/0008-5472.CAN-12-1702.
509 <http://www.ncbi.nlm.nih.gov/pubmed/23436801>

510 Mao, X., T. Cai, J.G. Olyarchuk, and L. Wei, 2005 Automated genome annotation and
511 pathway identification using the KEGG Orthology (KO) as a controlled vocabulary.
512 *Bioinformatics* 21 (19):3787-3793. doi:10.1093/bioinformatics/bti430.
513 <http://www.ncbi.nlm.nih.gov/pubmed/15817693>

514 Matsuda, E., O. Yu, and M. Kawaichi, 2008 CIBZ,a BTB-containing Zinc Finger
515 Protein,Plays a Role in Apoptosis and Tumorigenesis in *bit life sciences' 1st annual*
516 *world cancer congress-2008*.

517 Matsuoka, S., B.A. Ballif, A. Smogorzewska, E.R. McDonald, 3rd, K.E. Hurov *et al.*, 2007
518 ATM and ATR substrate analysis reveals extensive protein networks responsive to
519 DNA damage. *Science* 316 (5828):1160-1166. doi:10.1126/science.1140321.
520 <http://www.ncbi.nlm.nih.gov/pubmed/17525332>

521 McGettigan, P.A., 2013 Transcriptomics in the RNA-seq era. *Curr Opin Chem Biol* 17
522 (1):4-11. doi:10.1016/j.cbpa.2012.12.008.
523 <http://www.ncbi.nlm.nih.gov/pubmed/23290152>

524 Nishii, T., Y. Oikawa, Y. Ishida, M. Kawaichi, and E. Matsuda, 2012 CtBP-interacting BTB
525 zinc finger protein (CIBZ) promotes proliferation and G1/S transition in embryonic
526 stem cells via Nanog. *Journal of Biological Chemistry* 287 (15):12417.
527 doi:10.1074/jbc.M111.333856. <https://www.ncbi.nlm.nih.gov/pubmed/22315219>

528 Reimann, E., S. Koks, X.D. Ho, K. Maasalu, and A. Martson, 2014 Whole exome sequencing
529 of a single osteosarcoma case--integrative analysis with whole transcriptome
530 RNA-seq data. *Hum Genomics* 8:20. doi:10.1186/s40246-014-0020-0.
531 <http://www.ncbi.nlm.nih.gov/pubmed/25496518>

532 Robinson, M.D., D.J. McCarthy, and G.K. Smyth, 2010 edgeR: a Bioconductor package for
533 differential expression analysis of digital gene expression data. *Bioinformatics* 26
534 (1):139-140. doi:10.1093/bioinformatics/btp616.
535 <http://www.ncbi.nlm.nih.gov/pubmed/19910308>

536 Sasai, N., E. Matsuda, E. Sarashina, Y. Ishida, and M. Kawaichi, 2005 Identification of a
537 novel BTB-zinc finger transcriptional repressor, CIBZ, that interacts with CtBP
538 corepressor. *Genes to Cells* 10 (9):871–885. doi:10.1111/j.1365-2443.2005.00885.x.
539 <https://www.ncbi.nlm.nih.gov/pubmed/16115196>

540 Sawai, C.M., J. Freund, P. Oh, D. Ndiaye-Lobry, J.C. Bretz *et al.*, 2012 Therapeutic targeting
541 of the cyclin D3:CDK4/6 complex in T cell leukemia. *Cancer Cell* 22 (4):452-465.
542 doi:10.1016/j.ccr.2012.09.016. <http://www.ncbi.nlm.nih.gov/pubmed/23079656>

543 Shangary, S., and S. Wang, 2009 Small-molecule inhibitors of the MDM2-p53
544 protein-protein interaction to reactivate p53 function: a novel approach for cancer
545 therapy. *Annu Rev Pharmacol Toxicol* 49:223-241.
546 doi:10.1146/annurev.pharmtox.48.113006.094723.
547 <http://www.ncbi.nlm.nih.gov/pubmed/18834305>

548 Shi, Y., X. Gao, Q. Hu, X. Li, J. Xu *et al.*, 2016 PIK3C2A is a gene-specific target of
549 microRNA-518a-5p in imatinib mesylate-resistant gastrointestinal stromal tumor.
550 *Lab Invest* 96 (6):652-660. doi:10.1038/labinvest.2015.157.
551 <http://www.ncbi.nlm.nih.gov/pubmed/26950487>

552 Stogios, P.J., G.S. Downs, J.J. Jauhal, S.K. Nandra, and G.G. Prive, 2005 Sequence and
553 structural analysis of BTB domain proteins. *Genome Biol* 6 (10):R82.
554 doi:10.1186/gb-2005-6-10-r82. <http://www.ncbi.nlm.nih.gov/pubmed/16207353>

555 The, I., S. Ruijtenberg, B.P. Bouchet, A. Cristobal, M.B. Prinsen *et al.*, 2015 Rb and
556 FZR1/Cdh1 determine CDK4/6-cyclin D requirement in *C. elegans* and human
557 cancer cells. *Nat Commun* 6:5906. doi:10.1038/ncomms6906.
558 <http://www.ncbi.nlm.nih.gov/pubmed/25562820>

559 VanArsdale, T., C. Boshoff, K.T. Arndt, and R.T. Abraham, 2015 Molecular Pathways:
560 Targeting the Cyclin D-CDK4/6 Axis for Cancer Treatment. *Clin Cancer Res* 21
561 (13):2905-2910. doi:10.1158/1078-0432.CCR-14-0816.
562 <http://www.ncbi.nlm.nih.gov/pubmed/25941111>

563 Wang, D., M.A. Olman, J. Stewart, Jr., R. Tipps, P. Huang *et al.*, 2011 Downregulation of
564 FIP200 induces apoptosis of glioblastoma cells and microvascular endothelial cells
565 by enhancing Pyk2 activity. *PLoS One* 6 (5):e19629.
566 doi:10.1371/journal.pone.0019629. <http://www.ncbi.nlm.nih.gov/pubmed/21602932>

567 Wang, Z., M. Gerstein, and M. Snyder, 2009 RNA-Seq: a revolutionary tool for
568 transcriptomics. *Nat Rev Genet* 10 (1):57-63. doi:10.1038/nrg2484.
569 <http://www.ncbi.nlm.nih.gov/pubmed/19015660>

570 Wei, H., B. Gan, X. Wu, and J.L. Guan, 2009 Inactivation of FIP200 leads to inflammatory
571 skin disorder, but not tumorigenesis, in conditional knock-out mouse models. *J Biol
572 Chem* 284 (9):6004-6013. doi:10.1074/jbc.M806375200.
573 <http://www.ncbi.nlm.nih.gov/pubmed/19106106>

574 Young, M.D., M.J. Wakefield, G.K. Smyth, and A. Oshlack, 2010 Gene ontology analysis
575 for RNA-seq: accounting for selection bias. *Genome Biol* 11 (2):R14.
576 doi:10.1186/gb-2010-11-2-r14. <http://www.ncbi.nlm.nih.gov/pubmed/20132535>

577 Zhang, Z., J. Chen, F. Chen, D. Yu, R. Li *et al.*, 2017 Tauroursodeoxycholic acid alleviates
578 secondary injury in the spinal cord via up-regulation of CIBZ gene. *Cell Stress
579 Chaperones*. doi:10.1007/s12192-017-0862-1.
580 <http://www.ncbi.nlm.nih.gov/pubmed/29151236>

581 Zhao, Q.Y., Y. Wang, Y.M. Kong, D. Luo, X. Li *et al.*, 2011 Optimizing de novo
582 transcriptome assembly from short-read RNA-Seq data: a comparative study. *BMC*

583 *Bioinformatics* 12 Suppl 14:S2. doi:10.1186/1471-2105-12-S14-S2.
584 <http://www.ncbi.nlm.nih.gov/pubmed/22373417>

585